Interferometric lithography with an amplitude division interferometer and a desktop extreme ultraviolet laser

P. Wachulak,[1,2] M. Grisham,[1,2] S. Heinbuch,[1,2] D. Martz,[1,2] W. Rockward,[1,3] D. Hill,[1,3] J. J. Rocca,[1,2] C. S. Menoni,[1,2] E. Anderson,[1,4] and M. Marconi[1,2,*]

[1]*National Science Foundation Engineering Research Center for Extreme Ultraviolet Science & Technology, Colorado State University, 1373 Campus Delivery, Fort Collins, Colorado 80523, USA*

[2]*Department of Electrical and Computer Engineering, Colorado State University, 1373 Campus Delivery, Fort Collins, Colorado 80523, USA*

[3]*Morehouse College, 830 Westview Drive, SW, Atlanta, Georgia 30314, USA*

[4]*Center for X Ray Optics, Lawrence Berkeley National Laboratory, 1 Cyclotron Road, Berkeley, California 94720, USA*

**Corresponding author: Marconi@engr.colostate.edu*

Received December 12, 2007; revised March 5, 2008; accepted March 6, 2008;
posted March 31, 2008 (Doc. ID 90798); published May 21, 2008

We demonstrate a compact interferometric lithography nanopatterning tool based on an amplitude division interferometer (ADI) and a 46.9 nm wavelength desktop size capillary discharge laser. The system is designed to print arrays of lines, holes, and dots with sizes below 100 nm on high resolution photoresists for the fabrication of arrays of nanostructures with physical and biological applications. The future combination of this ADI with high repetition rate tabletop lasers operating at shorter wavelengths should allow the printing of arrays of sub-10 nm size features with a tabletop setup. © 2008 Optical Society of America

OCIS codes: 220.4241, 140.7240.

1. INTRODUCTION

The fabrication of large arrays of metallic or semiconductor pillars and holes with sizes below 100 nm has attracted attention due to their potential applications in several fields. These include, for example, the manufacturing of nanoscale rf oscillator arrays [1,2], patterned magnetic storage devices [3], and convenient devices for DNA sequencing [4]. Different approaches have been applied to the fabrication of arrays of nanoscale pillars and holes including electron beam lithography, self-assembly of nanospheres, or replication by embossing, molding, or printing with master stamps [5,6]. Electron beam lithography provides an outstanding spatial resolution capability but is a time consuming approach due to the intrinsic serial characteristic of the writing process [7]. The self-assembly approach permits the fabrication of large area periodic structures with nanometer size features; however special effort should be made in order to avoid dislocations, discontinuities, or the spontaneous generation of reduced size domains [8]. A very interesting alternative is replication with master stamps, a technique that has demonstrated feature sizes below 100 nm but requires a different master for each motif [9,10].

Interferometric lithography (IL) has emerged as an attractive maskless alternative to print in a relatively simple way arrays of nanoscale periodic features. This technique, which requires the use of a coherent light source, relies on the activation of a photoresist by the interference pattern generated by two or more mutually coherent light beams [11–17]. When two mutually coherent beams are combined in the surface of a photoresist, the generated interference pattern can activate the photoresist and print periodic lines with a period given by $p=\lambda/(2\sin\theta)$, where λ is the wavelength of the illumination and θ is the incidence angle. Several schemes can be implemented based on the same idea, but in all cases the ultimate resolution, $\lambda/2$, is limited by the wavelength of the illumination. Thus, reducing the wavelength is a direct path toward realizing interference patterns with dimensions of tens of nanometers and below. This characteristic has been the motivation for using extreme ultraviolet (EUV) and soft x-rays (SXR) synchrotron light for this application [15,18]. Feature sizes as small as 19 nm have been printed using a Lloyd's mirror interferometer with synchrotron illumination [17,18]. However, the widespread use of IL in nanotechnology applications would benefit from the implementation of more compact and easily accessible setups. The increased average power of compact plasma-based EUV lasers offers the possibility of implementing EUV IL on a tabletop. In recent work we demonstrated a compact nanopatterning system based on a Lloyd's mirror interferometer configuration illuminated with a 46.9 nm wavelength tabletop capillary discharge laser that allowed the printing of gratings and arrays of nanodots [19,20].

In this paper we describe a compact interferometric nanopatterning tool based on the combination of an amplitude division interferometer (ADI) and a desktop $\lambda=46.9$ nm capillary discharge laser. With interfering beams of equal path length and originating from the same

 © 2008 Optical Society of America

part of the wavefront, the ADI has significant advantages as compared with the wavefront division Lloyd's mirror configuration. First, with the ADI it is possible to print larger areas due to its relaxed spatial coherence requirements. This represents an important advantage, in particular when the interferometer is used in combination with laser-pumped tabletop EUV lasers that are not fully spatially coherent. In the ADI the interference in the sample plane is obtained by the superposition of two beams corresponding to the two branches that are replicas of the original wavefront impinging the beam splitter diffraction grating. Second, both beams have practically the same intensity and thus produce a higher and more uniform contrast in the interference pattern over the whole printed area.

2. EXPERIMENTAL DETAILS

For this initial demonstration of the ADI lithography tool we used an extremely compact, "desktop" $\lambda = 46.9$ nm Ne-like Ar capillary discharge laser configured to emit pulses with energy of $\sim 10\ \mu$J and ~ 1 ns FWHM duration. The EUV laser can operate at repetition rates up to 12 Hz producing pulses corresponding to average powers up to 0.12 mW. Due to its short capillary plasma column length (21 cm) its spatial coherence length is only a fraction of a millimeter at the sample location, a value that is significantly smaller than that corresponding to the tabletop capillary discharge laser used in previous Lloyd's mirror IL experiments [21,22]. The laser temporal coherence length is approximately 470 μm determined by its line width $\Delta\lambda/\lambda < 1 \times 10^{-4}$. The laser unit is extremely compact; it occupies a footprint of $0.8\ \text{m} \times 0.4\ \text{m}$ including its turbomolecular pump and has a small power supply that can fit under the optical table [23].

The ADI follows a Mach–Zehnder configuration, where the beam splitter is a transmission diffraction grating. Figure 1 shows a diagram of the interferometer and a photograph of the experimental setup with the paths of the two beams indicated by dashed curves. The 1 and −1 orders of the grating, that for the 46.9 nm illumination are separated by 2.68°, are used to form the two arms of the interferometer. The zero order is blocked from reaching the sample plane. The folding mirrors were implemented using two Si wafers placed at an incidence angle between 5° and 8° depending on the patterned period. The footprint of the interferometer is small, $\sim 0.2\ \text{m} \times 0.4\ \text{m}$. Its overall light throughput is at a maximum 6%, considering that the grating diffraction efficiency in the first order is 40.5%, the reflectivity of the Si mirrors is 94%, and the transparency of the Si membrane is 15%. The interference gives rise to a sinusoidal pattern of period p that is recorded on a hydrogen silsesquioxane (HSQ) photoresist deposited on a Si wafer.

The transmission grating used to split the beam has a 2 μm period with 50% duty cycle lines. It was fabricated in a $2\ \text{mm} \times 0.6\ \text{mm}$ Si membrane ~ 100 nm thick. Figure 2(a) schematically shows the sequence of steps in the grating fabrication process. A thin layer of Si was sputtered on top of a Si_3N_4 membrane fabricated in a 550 μm thick Si wafer. Subsequently, a 350 nm thick photoresist layer was deposited by spin coating on top of the sputtered Si. The grating was patterned in the photoresist by electron beam lithography. Finally, the Si_3N_4 layer was removed by chemically assisted ion beam etching through the substrate opening leaving a self-standing 100 nm thick Si membrane with the grating defined in the photoresist. The thin Si membrane provides 15%–20% transparency to the $\lambda = 46.9$ nm photons, while the photoresist that remains in the membrane acts as perfectly absorbent regions, constituting an amplitude transmission diffrac-

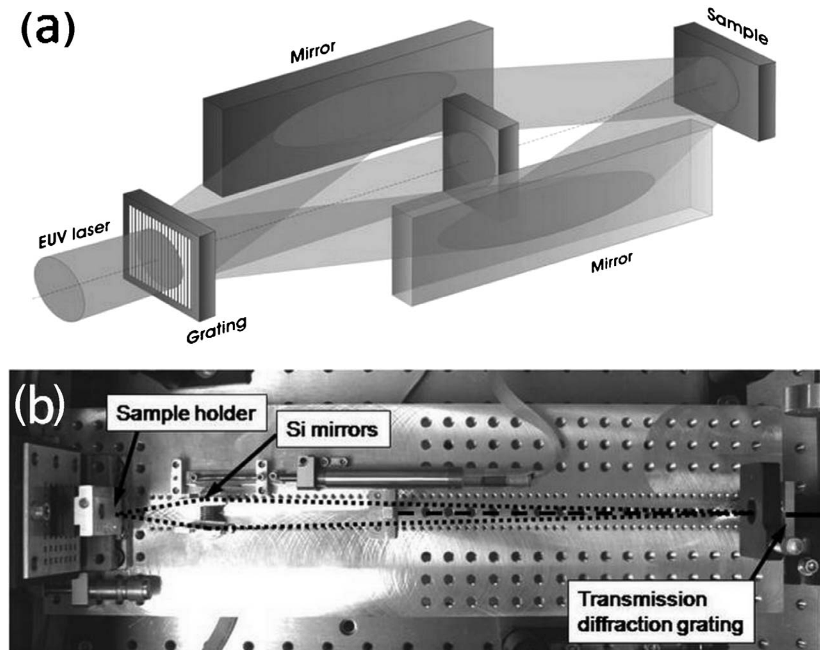

Fig. 1. (a) Schematic of the EUV ADI composed of a transmission diffraction grating beam splitter and a pair of grazing incidence mirrors. (b) Photograph of the setup. The dotted curves illustrate the optical paths of the two beams.

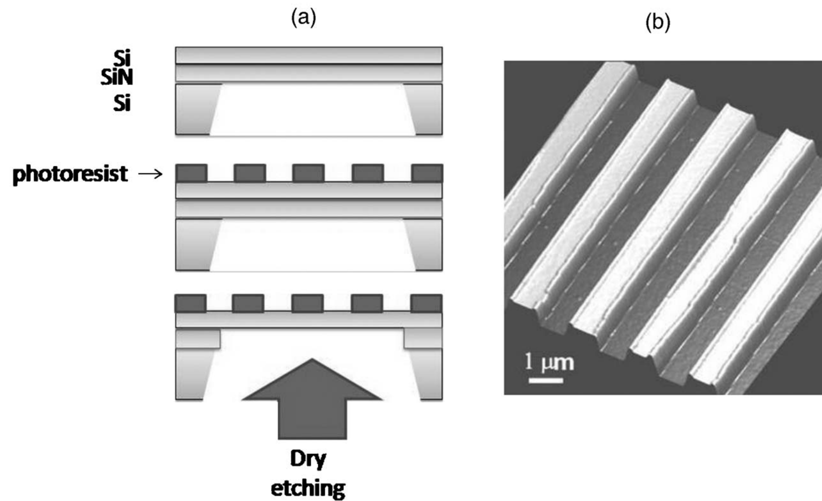

Fig. 2. (a) Sequence of steps for the fabrication of the transmission diffraction grating using electron beam lithography in a photoresist layer deposited on top of a 100 nm Si membrane. (b) AFM image of the transmission diffraction grating.

tion grating. Figure 2(b) shows an atomic force microscope (AFM) scan of the completed grating, revealing a highly regular profile. The resulting open areas were measured to be 980 nm wide and to have a period of 2.02 μm. The interferometer was positioned at 1.4 m from the exit of the capillary discharge plasma, where the laser beam uniformly illuminates the whole grating.

The optical path difference between the two branches of the interferometer can easily be adjusted within a distance smaller than 470 μm, the longitudinal coherence of the laser source. The required accuracy in the overlapping of the two beams at the sample's surface is defined by the spatial coherence of the beams, which for the $\lambda = 46.9$ nm laser used in this experiment is a fraction of a millimeter at the location of the sample. The system is very robust, requiring only minor adjustments after its initial alignment.

3. RESULTS

Figure 3(a) shows a dense line grating pattern with a period of 145 nm (72.5 nm thick lines) printed on the HSQ with the ADI setup. The printed area corresponds to the size of the grating beam splitter (in this experiment 2 mm × 0.6 mm). The penetration depth of the 46.9 nm light in the photoresist is ~120 nm. The images shown in Fig. 3 are AFM scans of the sample obtained with the AFM working in the tapping mode. To print gratings of a smaller period we increased the angle between the two beams impinging at the sample by changing the angle of incidence at the two Si mirrors and by correcting the position of the sample. A dense line pattern with an ~95 nm period (47.5 nm wide lines) printed on the HSQ over an area of 2 mm × 0.6 mm was obtained in this case. An AFM scan of this dense line pattern is shown in Fig. 3(b). Since the laser was operated at a repetition rate of only 3 Hz, exposures of more than 10 min were required. The exposures can be reduced by more than 1 order of magnitude by combining this ADI with the tabletop version of the capillary discharge laser (footprint 1 m × 0.5 m), which is capable of producing milliwatt average powers [21,22].

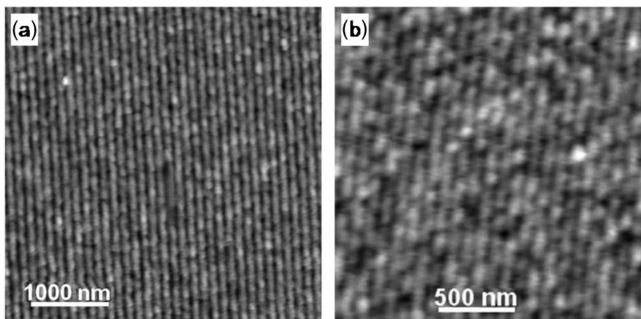

Fig. 3. (a) AFM image of a 145 nm period grating printed by IL using an EUV laser. (b) AFM image of a 95 nm period grating. Both images were obtained with the AFM working in the tapping mode over a small section of the printed grating.

The 95 nm period lines show an increased noise as compared with the larger pitch sample. One possible explanation for this lower quality printing is the influence of vibrations during the exposure. In addition the print quality may possibly be affected by photoresist scumming, which is particularly severe in 50% duty cycle lines with line widths approaching 50 nm [24] or by the presence of scattering centers in the grating and mirrors that introduce a random noise background reducing the fringe visibility.

The HSQ thickness in these experiments was 80 nm, which was set in order to match the measured penetration depth of the laser radiation in the photoresist and facilitate the subsequent processing of the substrate. The influence of the resist thickness in the spatial resolution was not evaluated at this time and will be the object of further investigation.

This proof-of-principle experiment can also be extended to demonstrate the printing of more complex two dimensional motifs, such as arrays of dots or holes. This can be realized by performing a second exposure after rotating the sample. The shape of the printed features can be altered by selecting the rotation angle and the exposure. This requires the incorporation of suitable rotation mechanisms for the sample similar to the experiment de-

scribed in [20]. Larger areas are also possible by either utilizing a transmission grating beam splitter of larger dimensions or by precisely translating the sample and realizing multiple exposures. Efforts are currently in progress in order to further develop this technique to print smaller and more complex features over larger areas using shorter wavelength lasers.

4. SUMMARY

In summary, we have demonstrated a compact EUV IL tool that combines an ADI with a desktop size EUV laser. In this proof-of-principle experiment we demonstrated the printing of gratings over areas of $2\,\text{mm} \times 0.6\,\text{mm}$ with periods down to 95 nm. As the average power of the shorter wavelength (e.g., 13.9 nm) high repetition rate tabletop EUV lasers increases, their combination with this interferometer will allow the printing of arrays with a sub-10 nm feature size on a tabletop [25]. These capabilities would enable the demonstration of a practical EUV IL tool for the fabrication of large arrays of periodic features that so far were restricted to the use of large synchrotron facilities.

ACKNOWLEDGMENTS

This work was supported by the National Science Foundation (NSF) Engineering Research Center (ERC) for extreme ultraviolet science and technology award EEC-0310717 and supplemental funding for collaborative research with Morehouse College.

REFERENCES

1. F. B. Mancoff, N. D. Rizzo, B. N. Engel, and S. Tehrani, "Phase-locking in double-point-contact spin-transfer devices," Nature **437**, 393–395 (2005).
2. A. N. Slavin and V. S. Tiberkevich, "Nonlinear self-phase-locking effect in an array of current-driven magnetic nanocontacts," Phys. Rev. B **72**, 092407 (2005).
3. F. Q. Zhu, D. L. Fan, X. C. Zhu, J. G. Zhu, R. C. Cammarata, and C. L. Chien, "Ultrahigh-density arrays of ferromagnetic nanorings on macroscopic areas," Adv. Mater. (Weinheim, Ger.) **16**, 2155–2159 (2004).
4. M. J. Kim, M. Wanunu, D. C. Bell, and A. Meller, "Rapid fabrication of uniformly sized nanopores and nanopore arrays for parallel DNA analysis," Adv. Mater. (Weinheim, Ger.) **18**, 3149–3153 (2006).
5. S. Y. Chou, "Nanoimprint lithography and lithographically induced self-assembly," MRS Bull. **26**, 512–517 (2001).
6. H. Schulz, D. Lyebyedyev, H. C. Scheer, K. Pfeiffer, G. Bleidiessel, G. Grutzner, and J. Ahopelto, "Master replication into thermosetting polymers for nanoimprinting," J. Vac. Sci. Technol. B **18**, 3582–3585 (2000).
7. E. H. Anderson, "Specialized electron beam nanolithography for EUV and x-ray diffractive optics," IEEE J. Quantum Electron. **42**, 27–35 (2006).
8. S. O. Kim, H. H. Solak, M. P. Stoykovich, N. J. Ferrier, J. J. de Pablo, and P. F. Nealey, "Epitaxial self-assembly of block copolymers on lithographically defined nanopatterned substrates," Nature **424**, 411–414 (2003).
9. S. Y. Chou and P. R. Krauss, "Imprint lithography with sub-10 nm feature size and high throughput," Microelectron. Eng. **35**, 237–240 (1997).
10. S. Y. Chou, P. R. Krauss, and P. J. Renstrom, "Nanoimprint lithography," J. Vac. Sci. Technol. B **14**, 4129–4133 (1996).
11. S. R. J. Brueck, "Optical and interferometric lithography—nanotechnology enablers," Proc. IEEE **93**, 1704–1721 (2005).
12. A. Fernandez, J. Y. Decker, S. M. Herman, D. W. Phillion, D. W. Sweeney, and M. D. Perry, "Methods for fabricating arrays of holes using interference lithography," J. Vac. Sci. Technol. B **15**, 2439–2443 (1997).
13. W. Hinsberg, F. A. Houle, J. Hoffnagle, M. Sanchez, G. Wallraff, M. Morrison, and S. Frank, "Deep-ultraviolet interferometric lithography as a tool for assessment of chemically amplified photoresist performance," J. Vac. Sci. Technol. B **16**, 3689–3694 (1998).
14. J. A. Hoffnagle, W. D. Hinsberg, M. Sanchez, and F. A. Houle, "Liquid immersion deep-ultraviolet interferometric lithography," J. Vac. Sci. Technol. B **17**, 3306–3309 (1999).
15. H. H. Solak and C. David, "Patterning of circular structure arrays with interference lithography," J. Vac. Sci. Technol. B **21**, 2883–2887 (2003).
16. H. H. Solak, C. David, J. Gobrecht, L. Wang, and F. Cerrina, "Multiple-beam interference lithography with electron beam written gratings," J. Vac. Sci. Technol. B **20**, 2844–2848 (2002).
17. H. H. Solak, D. He, W. Li, and F. Cerrina, "Nanolithography using extreme ultraviolet lithography interferometry: 19 nm lines and spaces," J. Vac. Sci. Technol. B **17**, 3052–3057 (1999).
18. H. H. Solak, D. He, W. Li, S. Singh-Gasson, F. Cerrina, B. H. Sohn, X. M. Yang, and P. Nealey, "Exposure of 38 nm period grating patterns with extreme ultraviolet interferometric lithography," Appl. Phys. Lett. **75**, 2328–2330 (1999).
19. M. G. Capeluto, G. Vaschenko, M. Grisham, M. C. Marconi, S. Luduena, L. Pietrasanta, Y. F. Lu, B. Parkinson, C. S. Menoni, and J. J. Rocca, "Nanopatterning with interferometric lithography using a compact lambda=46.9-nm laser," IEEE Trans. Nanotechnol. **5**, 3–7 (2006).
20. P. W. Wachulak, M. G. Capeluto, M. C. Marconi, C. S. Menoni, and J. J. Rocca, "Patterning of nano-scale arrays by table-top extreme ultraviolet laser interferometric lithography," Opt. Express **15**, 3465–3469 (2007).
21. B. R. Benware, C. D. Macchietto, C. H. Moreno, and J. J. Rocca, "Demonstration of a high average power tabletop soft x-ray laser," Phys. Rev. Lett. **81**, 5804–5807 (1998).
22. C. D. Macchietto, B. R. Benware, and J. J. Rocca, "Generation of millijoule-level soft-x-ray laser pulses at a 4-Hz repetition rate in a highly saturated tabletop capillary discharge amplifier," Opt. Lett. **24**, 1115–1117 (1999).
23. S. Heinbuch, M. Grisham, D. Martz, and J. J. Rocca, "Demonstration of a desk-top size high repetition rate soft x-ray laser," Opt. Express **13**, 4050–4055 (2005).
24. D. P. Mancini, K. A. Gehoski, E. Ainley, K. J. Nordquist, D. J. Resnick, T. C. Bailey, S. V. Sreenivasan, J. G. Ekerdt, and C. G. Willson, "Hydrogen silsesquioxane for direct electron-beam patterning of step and flash imprint lithography templates," J. Vac. Sci. Technol. B **20**, 2896–2901 (2002).
25. Y. Wang, M. A. Larotonda, B. M. Luther, D. Alessi, M. Berrill, V. N. Shlyaptsev, and J. J. Rocca, "Demonstration of high-repetition-rate tabletop soft-x-ray lasers with saturated output at wavelengths down to 13.9 nm and gain down to 10.9 nm," Phys. Rev. A **72**, 053807 (2005).